Patel, D. J., Kozlowski, S. A., Marky, L. A., Rice, J. A., Broka, C., Itakura, K., & Breslauer, K. J. (1982) *Biochemistry 21*, 445–451.
Redfield, A. G., Kunz, S. D., & Ralph, E. K. (1975) *J. Magn. Reson. 19*, 114–117.
Sanchez, V., Redfield, A. G., Johnston, P. D., & Tropp, J. (1980) *Proc. Natl. Acad. Sci. U.S.A. 77*, 5659–5662.
Streisinger, G., Okada, Y., Emrich, J., Newton, J., Tsugita, A., Terzaghi, E., & Inouye, M. (1966) *Cold Spring Harbor Symp. Quant. Biol. 31*, 77–84.
Uhlenbeck, O. C., Borer, P. N., Dengler, B., & Tinoco, I., Jr. (1973) *J. Mol. Biol. 73*, 497–511.
Wagner, G., Pardi, A., & Wüthrich, K. (1983) *J. Am. Chem. Soc. 105*, 5948–5949.

Internal Motions in Ribonucleic Acid Duplexes As Determined by Electron Spin Resonance with Site-Specifically Spin-Labeled Uridines†

Shih-Chung Kao, Carl F. Polnaszek, Charles R. Toppin, and Albert M. Bobst*

ABSTRACT: We have used site-specifically spin-labeled polyribonucleotides to extract motional information for single- and double-stranded polyribonucleotides. The spin-label is attached to either position 4 or 5 of an uridine analogue, and in the latter position the label is linked through various tethers to the base. This strategy together with a motional model has allowed us to separate the motion of the base from the motion of the spin-label in single and double strands. We conclude that the bases in an RNA duplex experience substantial motions with a correlation time in the range of 4 ns.

Internal motions of nucleic acid duplexes have been studied by a variety of techniques (Bolton & James, 1979; Feigon & Kearns, 1979; Klevan et al., 1979; Bobst, 1980; Hogan & Jardetzky, 1980; Robinson et al., 1980a,b; Shido & McGhee, 1980; Bobst et al., 1981a; Hogan et al., 1982; Allison et al., 1982; Hurley et al., 1982; McCain et al., 1982; Wang et al., 1982). Phosphate backbone motion of DNA in nucleosomes occurs with a time constant of 1–30 ns as determined by ^{31}P NMR (Klevan et al., 1979; Shindo & McGhee, 1980), but a rigid DNA in nucleosomes was derived on the basis of ^{1}H NMR line-width measurements (Feigon & Kearns, 1979). More recently substantial DNA motions with a time constant near 30 ns in nucleosomes and histone-free DNA were determined by triplet anisotropy decay of intercalating dyes (Hogan et al., 1982; Wang et al., 1982). Similar mobilities were derived from ESR measurements on spin labeled propidium intercalated in DNA which resulted in correlation times of the order of 30 ns (Robinson et al., 1980a,b; Hurley et al., 1982).

We present results about the motions of single-stranded and double-stranded polyribonucleotides based on site-specifically spin-labeled nucleic acid building blocks. The spin-label, consisting of a six-membered nitroxide radical with tethers of variable lengths, is attached in either position 4 or 5 of the pyrimidine base. In the latter position various tethers are used to attach the nitroxide radical to the base. With this strategy we were able to express the ESR line shapes in terms of geometrical (tilt angle) and two motional parameters ($\tau_{\parallel}$ and $\tau_{\perp}$),[1] thereby allowing us to separate the motion of the tether axis from motions due to torsion and tilting of the base pairs as well as twisting of the bases. We conclude that the motions of the bases in an RNA duplex occur in the range of 4 ns.

Materials and Methods

$(A)_n$ was bought from P-L Biochemicals (minimum s_{20}) and purified through Sephacryl S-200 prior to use. All other materials were commercial products of analytical reagent grade.

Synthesis of $(pps^5U)_2$. A sulfur substituent was introduced into position 5 of uridine 5′-diphosphate according to a published procedure (Ho et al., 1978). The 5-thiolated nucleotide disulfide was isolated as the ammonium salt in overall 20–30% yield and was characterized by its UV spectrum (λ_{max}^{pH7} = 273 nm) (Ho et al., 1978).

Preparation of Spin-Labeled Alkylating Agents. Epoxy-Tempo, the synthesis of which was reported earlier by others (Rauckman et al., 1976), was obtained in small quantities from Molecular Probes, Inc. (Junction City, OR), and in larger quantities from the Josef Stefan Institut in Yugoslavia. α-Iodoacetamido-Tempo was isolated after activation of the

† From the Department of Chemistry, University of Cincinnati, Cincinnati, Ohio 45221 (S.-C.K., C.R.T., and A.M.B.), and the Department of Chemistry, University of Minnesota, Minneapolis, Minnesota 55455 (C.F.P.). *Received May 9, 1983.* This investigation was supported in part by grants from the U.S. National Science Foundation (No. PCM 7801979) and U.S. Public Health Service (No. GM 27002). Purchase of the Nicolet NTC 300 FT instrument was supported in part by National Science Foundation Grant CHE-81-02974.

[1] Abbreviations: $(A)_n$, poly(adenylic acid); $(U)_n$, poly(uridylic acid); $(pps^5U)_2$, bis[1-(5′-*O*-diphosphono-β-D-ribofuranosyl)uracil-5-yl] disulfide; epoxy-Tempo, 5,5,7,7-tetramethyl-1-oxa-6-azaspiro[2.5]oct-6-yloxy; α-iodoacetamido-Tempo, 4-(α-iodoacetamido)-2,2,6,6-tetramethylpiperidinyl-1-oxy; β-iodopropanamido-Tempo, 4-(β-iodopropanamido)-2,2,6,6-tetramethylpiperidinyl-1-oxy; DTT, dithiothreitol; $(RUMMT,U)_n$, copolymer of RUMMT and uridine; ppRUMMT, (1-oxy-2,2,6,6-tetramethyl-4-hydroxy-4-piperidinyl)methyl 1-(5′-*O*-diphosphono-β-D-ribofuranosyl)uracil-5-yl sulfide; $(RUTT,U)_n$, copolymer of RUTT and uridine; ppRUTT, *N*-[(1-oxy-2,2,6,6-tetramethyl-4-piperidinyl)methyl]carbamoyl 1-(5′-*O*-diphosphono-β-D-ribofuranosyl)-uracil-5-yl sulfide; $(RUMPT,U)_n$, copolymer of RUMPT and uridine; ppRUMPT, *N*-[(1-oxy-2,2,6,6-tetramethyl-4-piperidinyl)ethyl]carbamoyl 1-(5′-*O*-diphosphono-β-D-ribofuranosyl)uracil-5-yl sulfide; $(1s^4U,U)_n$, copolymer of $1s^4U$ and uridine; pp$1s^4U$, *N*-[(1-oxy-2,2,6,6-tetramethyl-4-piperidinyl)methyl]carbamoyl 1-(5′-*O*-diphosphono-β-D-ribofuranosyl)uracil-4-yl sulfide; RNA, ribonucleic acid; T_m^{OD}, melting temperature determined by UV spectroscopy; $\tau_{\parallel}$ and $\tau_{\perp}$, correlation times for rotations about and perpendicular to the principal axis of diffusion, respectively.

0006-2960/83/0422-5563$01.50/0

chlorinated derivative (Eastman) by sodium iodide in anhydrous acetone (Ozinskas & Bobst, 1979).

4-(β-Chloropropanamido)-2,2,6,6-tetramethylpiperidinyl-1-oxy was synthesized by condensation of 1.2 mmol of 3-chloropropanoic acid (Aldrich) with an equimolar amount of 4-amino-2,2,6,6-tetramethylpiperidinyl-1-oxy (Eastman) in the presence of 1.3 mmol of *N,N'*-dicyclohexylcarbodiimide (Aldrich) in 4 mL of dichloromethane. The reaction mixture was stirred at 4 °C in the absence of light for 5 days. The desired product was isolated by preparative TLC (R_f 0.40; methanol–chloroform, 1:19 v/v) in 82% yield: mass spectrum, m/z 261 for M^+. The activated alkylating agent β-iodopropanamido-Tempo was obtained after reaction with a 1.4 molar excess of sodium iodide at 50 °C in anhydrous acetone for 2 days and used without isolation for the preparation of ppRUMPT.

Synthesis of ppRUMMT. To 0.016 mmol of $(pps^5U)_2$ in 0.2 mL of 0.5 M KH_2PO_4 buffer (pH 7.8) was added 0.025 mmol of DTT (Sigma). After the reaction mixture was stirred for 30 min at room temperature, 0.032 mmol of epoxy-Tempo in 0.20 mL of acetone was added, and stirring was continued for 6 h. More DTT and alkylating agent were added over the course of the reaction such that the final amount of the former present was 0.1 mmol and of the latter was 0.13 mmol. The desired material was isolated by preparative paper chromatography with Whatman 3MM paper (absolute ethanol–1 M ammonium acetate, 7:3 v/v) and repurified on a DEAE-Sephadex ion-exchange column with a linear gradient of 0.05–0.4 M NH_4HCO_3. Final purification was achieved on a Synchropak AX 300 (Synchrom) analytical HPLC column. The identity of the nucleoside structure was established from ^1H NMR in D_2O after reduction of the nitroxide with sodium dithionite (Ozinskas & Bobst, 1980). Tetramethylammonium chloride was used as standard and assigned the value of δ 3.0. The nonexchangeable hydrogen resonances of the reduced 5'-monophosphate of RUMMT are the following: C6-H, δ 8.1 (s); CH_2 (exocyclic), δ 2.7 (s); CH_2 (piperidine), δ 1.7 (m); CH_3 (piperidine), δ 1.2 (s) and 1.5 (s); C1'-H, δ 5.8 (d); C2'-H to C5'-H, δ 3.7–4.3 (m).

Synthesis of ppRUTT. The conditions for the synthesis of ppRUTT have been described (Toppin, 1983).

Synthesis of ppRUMPT. $(pps^5U)_2$ was alkylated under the same conditions as used for ppRUMMT with β-iodopropanamido-Tempo instead of epoxy-Tempo as alkylating agent. ppRUMPT had also like ppRUMMT to be purified over HPLC. The nonexchangeable hydrogen resonances of the reduced 5'-monophosphate of RUMPT are the following: C6-H, δ 8.0 (s); CH_2 (exocyclic, adjacent to sulfur), δ 2.7 (m); CH_2 (exocyclic, adjacent to carbonyl), δ 2.4 (m); CH (piperidine), δ 2.9 (m); CH_2 (piperidine), δ 1.8 (t); CH_3 (piperidine), δ 1.2 (s) and 1.3 (s); C1'-H, δ 5.8 (d); C2'-H to C5'-H, δ 3.8–4.5 (m).

Synthesis of pp1s^{4}U. The position 4 spin-labeled uridine 5'-diphosphate analogue was synthesized according to a previously described procedure (Warwick et al., 1980). The nonexchangeable hydrogen resonances of the reduced 5'-monophosphate of 1s^{4}U are the following: C5-H, δ 6.5 (d); C6-H, δ 8.1 (d); CH_2 (exocyclic) and CH (piperidine), δ 3.7–4.4 (m); CH_2 (piperidine), δ 1.8 (d); CH_3 (piperidine), δ 1.2 (s) and 1.3 (s); C1'-H, δ 5.8 (m); C2'-H to C5'-H, δ 3.7–4.4 (m).

Enzymatic Synthesis of Spin-Labeled RNA. $(1s^4U,U)_n$ was prepared according to a published procedure (Warwick et al., 1980). All other spin-labeled RNAs were prepared under conditions similar to those described for $(1s^4U,U)_n$ by copolymerizing uridine 5'-diphosphate with the appropriate nitroxide-containing nucleoside 5'-diphosphate analogue. All spin-labeled polyribonucleotides were isolated and characterized by the techniques mentioned earlier (Hakam et al., 1980). Their weight-average molecular weight was 100 000–200 000 and the nitroxide-labeled nucleotide to unmodified nucleotide ratio was 1 to 2%.

The UV absorbance thermal denaturation measurements were done with a Gilford 250 spectrophotometer and a Gilford 2527 thermoprogrammer by using a cell assembly consisting of four quartz microcells in an electrically heated block at a heating rate of 1 °C/min.

The ESR spectra were recorded with a Varian E-104 spectrometer interfaced to an Apple II plus microcomputer. The ESR spectral simulations were carried out on an Amdahl 470 computer (U.C.) and a CDC Cyber 74 (U.M.) with typical CPU times of 10 s/spectrum for the conditions given in Table II. An Apple II plus microcomputer interfaced to a Houston Instrument DMP-3 digital plotter was used to plot the simulated spectra to scale.

The NMR spectra were obtained on a Nicolet NTC 300 FT instrument and the electron impact mass spectra on a Perkin-Elmer RMU-7 spectrometer.

Theory

The spectra of the spin-labeled RNA systems were fitted by means of slow motional line-shape calculations [see Freed (1976) for an overall review]. This approach was chosen over the "fast motion" analysis of Polnaszek et al. (1978) used by Luoma et al. (1982) for spin-labeled RNA spectra, because one or more of the correlation times (τ) for the nitroxide motion are longer than 3 ns [the upper limit of validity of the fast motion theory (Goldman et al., 1972; Polnaszek & Freed, 1975)]. In fact, for spin-labeled RNA a line-shape simulation gave a value of 20 ns (Luoma et al., 1982).

Often the principal axis of diffusion z' determined by the structure of the molecule is not coincident to one of the principal axes of the nitroxide (x, y, and z in Figure 2) (Mason et al., 1974; Robinson & Dalton, 1980). In this case additional terms must be added to the line-shape equations given in Appendix A of Freed (1976). Robinson & Dalton (1980) and Meirovitch et al. (1982) have given equivalent equations. In the present model the usual assumption (Griffith et al., 1965; Berliner, 1976) that the axes of the **g** and hyperfine tensors are coincident has been made. Also, in spin-label studies of nonoriented systems at 9 GHz, the motion is most sensitive to only one tilt angle as the anisotropy of the hyperfine interaction in the x–y plane is quite small (Griffith et al., 1965; Berliner, 1976) and the resultant line shapes are insensitive to the second tilt angle which involves the x axis.

The rotational motion of the molecule is characterized by two correlation times, $\tau_\parallel$ for motions about the principal axis of diffusion z' and $\tau_\perp$ for motions about the two orthogonal diffusion axes of the molecule; i.e., the diffusion tensor is axially symmetric. The tilt angle between the diffusion and magnetic axes is defined as follows: One of the axes for $\tau_\perp$ is chosen coincident with the magnetic y axis. The principal axis of diffusion z' is initially coincident with the magnetic z axis. The diffusion axis z' is then rotated about the y axis by the tilt angle [see Figure 1 of Robinson & Dalton (1980)]. This also corresponds to a rotation of the other $\tau_\perp$ axis by the tilt angle with respect to the magnetic x axis. The spectra are invariant to the sign of the tilt angle, and because of symmetry, unique spectra are obtained only for the range of 0–90°. The magnetic axes can be permuted as in Goldman et al. (1972) to tilt the diffusion tensor with respect to any of the principal

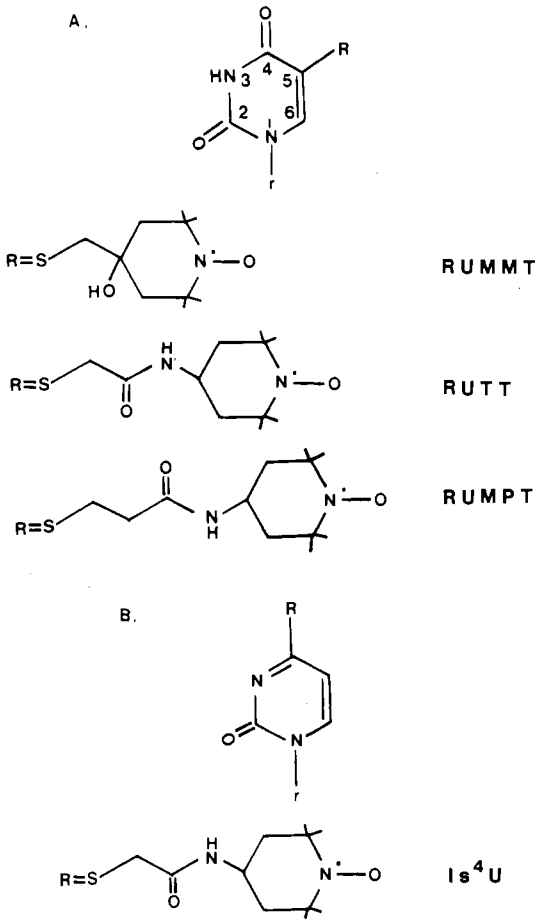

FIGURE 1: (A) 5-Substituted and (B) 4-substituted spin-labeled nucleic acid building blocks.

magnetic axes. Thus, the program requires one additional input parameter, the tilt angle, compared to that given in Freed (1976). The terminating values for the expansion parameters L and K in the line-shape calculation (Freed, 1976) are determined by the larger of $\tau_{\parallel}$ and $\tau_{\perp}$.

The tilt program used by Mason et al. (1974) has been modified to include odd L states. Polnaszek (1976) examined the effect of the inclusion of terms with odd L values on the ESR spectra for isotropic motion ($\tau_{\parallel} = \tau_{\perp}$) and no tilt angle. It was found that there were no differences in the spectra with and without odd L values for values of $\tau \leq 10^{-8}$ s. For values of $\tau \geq 5 \times 10^{-8}$ s noticeable differences were observed on the low-field part of the central line.

For the spin-labeled RNA systems the parameters are chosen as shown in Figure 2. The bond between the base and the sulfur atom was selected as the principal rotational diffusion axis z'. The tilt angle is the angle between this axis and the nitroxide z axis. In this model $\tau_{\parallel}$ corresponds to the motion of the tether axis about the z' axis, whereas $\tau_{\perp}$ reflects motions due to torsions and tilting of the base pairs as well as twisting of the bases. A similar model has been used to analyze the motion of a spin-labeled polymer (Mason et al., 1974). Thus, $\tau_{\perp}$ is the physically important parameter for the analysis of spin-labeled RNA motion which can be quantitated by using the slow motional theory.

The values of the spin parameters A_{xx}, A_{yy}, A_{zz}, g_{xx}, g_{yy}, and g_{zz} are those used earlier for spin-labeled nucleic acid systems (Bobst, 1979). The additional line-broadening term T_2^{-1} to account for broadening by the unresolved proton splittings and other interactions which do not depend upon the motion was determined by fitting the central line of the experimental spectra. The spectra were calculated at 5° increments of the tilt angle for various combinations of $\tau_{\parallel}$ and $\tau_{\perp}$ to form a library of theoretical line shapes.

Results

The structures of the 5-substituted and 4-substituted spin-labeled nucleic acid building blocks are shown in parts A and B of Figure 1, respectively. The size of the tether increases in the case of the 5-substituted derivatives by two bonds from RUMMT to RUTT and by an additional bond from RUTT to RUMPT. The 4-substituted derivative, $1s^4U$, has the same tether length as RUTT. Furthermore, in all cases the tether links the six-membered nitroxide radical via a sulfur bridge to the base. This pyrimidine sulfur linkage is defined as the principal rotational diffusion axis z' (Figure 2).

The physical properties of the spin-labeled duplexes $(RUMMT,U)_n(A)_n$, $(RUTT,U)_n(A)_n$, and $(RUMPT,U)_n(A)_n$ were monitored by UV absorbance melting experiments. The T_m^{OD} of the spin-labeled RNA duplexes and of $(U)_n(A)_n$ was for all duplexes 51 ± 0.5 °C, and this finding corroborates our earlier observations. Namely, we reported earlier for

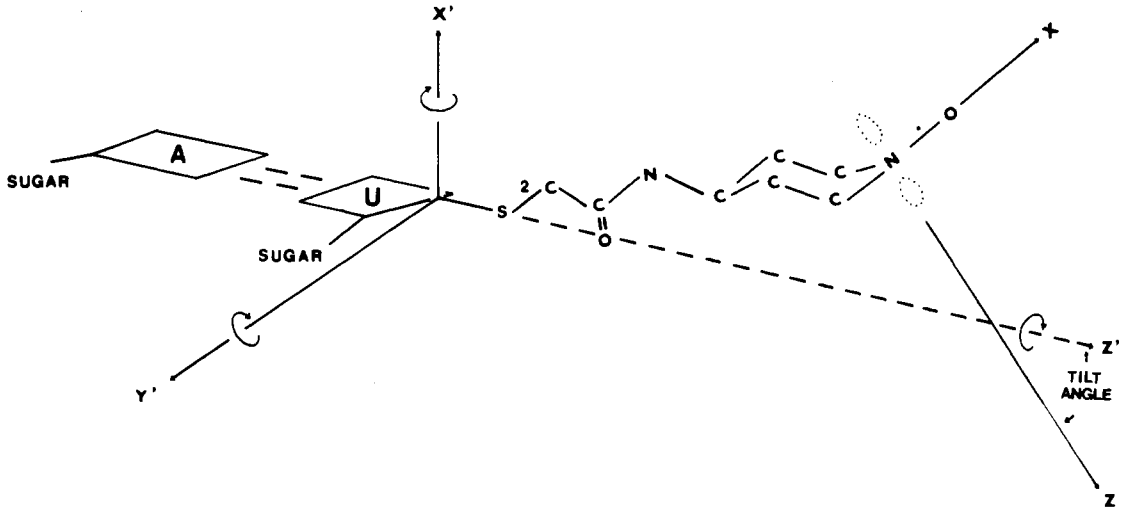

FIGURE 2: Schematic diagram of RUTT base paired with A. A stands for adenine and U for uridine. The principal rotational diffusion axis z' is tilted by an angle with respect to the molecular hyperfine principal z axis. $\tau_{\parallel}$ is the correlation time for rotation about the z' axis, and $\tau_{\perp}$ is the correlation time for rotation about an axis (x' or y' axis) perpendicular to the z' axis. For simplicity the methyl groups of the nitroxide ring are not shown.

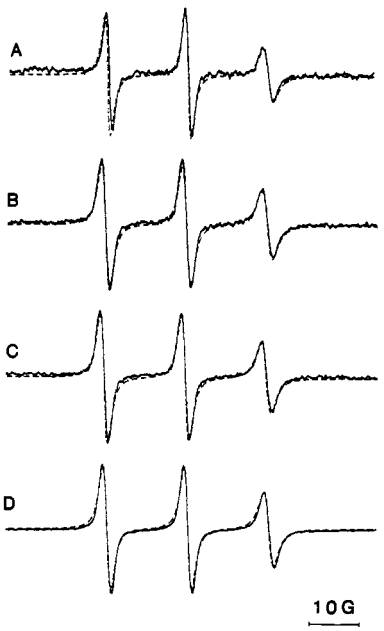

FIGURE 3: Experimental (—) and computer-simulated (---) ESR spectra of spin-labeled single strands. The displayed experimental spectra were taken in 0.01 M NaCl and 0.01 M sodium cacodylate, pH 7. (A) 2.3×10^{-4} M $(RUMMT,U)_n$; (B) 2.3×10^{-4} M $(RUTT,U)_n$; (C) 2.3×10^{-4} M $(RUMPT,U)_n$; (D) 1.2×10^{-4} M $(1s^4U,U)_n$. The computer-simulated spectra were obtained as described in the text with parameters given in Table I.

Table I: Effect of Tether Length of Label on Motion for Single-Stranded Systems[a]

single-stranded system	$\tau_\parallel$ (ns)	$\tau_\perp$ (ns)	tilt angle (deg)
$(RUMMT,U)_n$	0.1	1.2	45
$(RUTT,U)_n$	0.09	1.2	55
$(RUMPT,U)_n$	0.08	1.2	55
$(1s^4U,U)_n$	0.07	1.2	55

[a] Nitroxide ESR parameters: $A_{xx} = 7.15$ G; $A_{yy} = 7.35$ G; $A_{zz} = 35.6$ G; $g_{xx} = 2.0088$; $g_{yy} = 2.0059$; $g_{zz} = 2.0026$. Additional line broadening (T_2^{-1}): 0.8 G for $(RUMMT,U)_n$; 1.2 G for $(RUTT,U)_n$, $(RUMPT,U)_n$, and $(1s^4U,U)_n$.

$(RUGT,U)_n(A)_n$ (Langemeier & Bobst, 1981) that the perturbation of enzymatically incorporated nitroxide radicals on the thermal stability of RNA duplexes is minimal, if at all, since the T_m^{OD} of the spin-labeled duplexes was very similar to that of $(U)_n(A)_n$.

The experimental and computer-simulated ESR spectra of the single-stranded spin-labeled $(U)_n$ derivatives $(RUMMT,U)_n$, $(RUTT,U)_n$, $(RUMPT,U)_n$, and $(1s^4U,U)_n$ are shown in Figure 3. All four spectra display essentially the same line shapes which are characteristic for a nitroxide label undergoing rapid motion. The parameters used for the computer simulation of the spin-labeled single strands are listed in Table I. The tilt angle is on the order of 55 ± 5° for all except $(RUMMT,U)_n$ which has a smaller angle of 45 ± 5°. This smaller tilt angle is believed to reflect the effect of the additional hydroxide group in the six-membered ring of the RUMMT label.

$\tau_\parallel$ reflecting the motion of the tether axis is on the order of 0.07–0.1 ns in all cases and is about 12 times faster than $\tau_\perp$ which is 1.2 ns for the spin-labeled single strands. It is interesting to note that the mobility of the label does not depend on the labeling position in the single strands in contrast to the strong effect of the labeling position for double strands as is shown below.

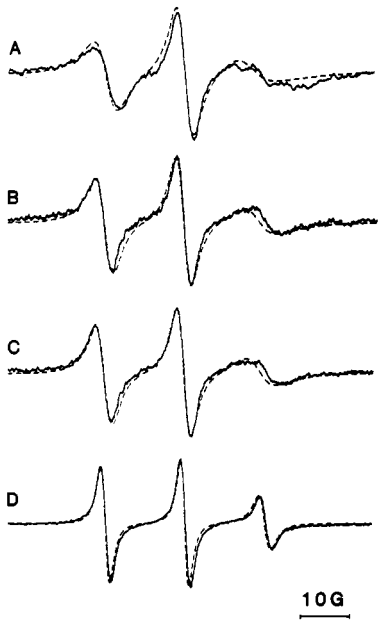

FIGURE 4: Experimental (—) and computer-simulated (---) ESR spectra of spin-labeled double strands. The displayed experimental spectra were obtained in 0.01 M NaCl and 0.01 M sodium cacodylate, pH 7. (A) 4.6×10^{-4} M $(RUMMT,U)_n(A)_n$; (B) 4.6×10^{-4} M $(RUTT,U)_n(A)_n$; (C) 4.6×10^{-4} M $(RUMPT,U)_n(A)_n$; (D) 2.4×10^{-4} M $(1s^4U,U)_n(A)_n$. The computer-simulated spectra were obtained as described in the text with parameters given in Table II.

Table II: Effect of Tether Length of Label on Motion for Double Strands[a]

double-stranded systems	$\tau_\parallel$ (ns)	$\tau_\perp$ (ns)	tilt angle (deg)
$(RUMMT,U)_n(A)_n$	2	4	80
$(RUTT,U)_n(A)_n$	0.5	4	40
$(RUMPT,U)_n(A)_n$	0.4	4	40
$(1s^4U,U)_n(A)_n$	0.1	1.2	40

[a] Nitroxide ESR parameters for $(RUMMT,U)_n(A)_n$: $A_{xx} = 7.35$ G; $A_{yy} = 35.6$ G; $A_{zz} = 7.15$ G; $g_{xx} = 2.0059$; $g_{yy} = 2.0026$; $g_{zz} = 2.0088$. Additional line broadening (T_2^{-1}): 0.4 G. Nitroxide ESR parameters for $(RUTT,U)_n(A)_n$, $(RUMPT,U)_n(A)_n$, and $(1s^4U,U)_n(A)_n$: $A_{xx} = 7.15$ G; $A_{yy} = 7.35$ G; $A_{zz} = 35.6$ G; $g_{xx} = 2.0088$; $g_{yy} = 2.0059$; $g_{zz} = 2.0026$. Additional line broadening (T_2^{-1}): 0.8 G for $(RUTT,U)_n(A)_n$ and $(RUMPT,U)_n(A)_n$; 1.0 G for $(1s^4U,U)_n(A)_n$.

In Figure 4 the experimental and computer-simulated ESR spectra of the double strands $(RUMMT,U)_n(A)_n$, $(RUTT,U)_n(A)_n$, $(RUMPT,U)_n(A)_n$, and $(1s^4U,U)_n(A)_n$ are shown. The ESR spectra of the duplexes are considerably broadened as compared to those of the single strands and reveal tether as well as position specificity. The spin-labeled duplex with the smallest tether, $(RUMMT,U)_n(A)_n$ has the most broadened line shape, whereas the duplex $(1s^4U,U)(A)_n$ displays three relatively narrow signals. The measurement of the former spectrum involved 32 scans of accumulation and the latter one only four. The small dip to the right of the high-field transition in Figure 4A could possibly arise from some weak cavity signal apparent with substantial time averaging, and this could account for the relatively poor fit of the high-field transition. The simulations of the ESR spectra were achieved with the parameters given in Table II. The tilt angles are for all on the order of 40 ± 5° except for the duplex containing RUMMT, which gives a larger tilt angle of 80 ± 5°. A comparison of the tilt angles between single and double strands reveals that complex formation results in the largest tilt angle change for the label closest to the base, i.e., about 35° for

RUMMT. $\tau_\perp$ which is believed to reflect the base mobility is about 4 ns for all 5-substituted nucleic acid building blocks, whereas $\tau_\perp$ is about 3 times faster for the 4-substituted derivative. $\tau_\parallel$ is tether dependent and gives the largest value for the shortest tether. Although the simulation solutions are not unique if each system would be considered individually, there seems to be only one solution fitting the model used to analyze all the different systems examined here.

Discussion

It has been shown that DNA duplexes possess substantial internal fluctuations which are postulated to be intrinsic to the structure of DNA (Hogan et al., 1982; Wang et al., 1982). A model to understand the internal rotations in a spin-labeled protein was developed earlier (Wallach, 1967) to relate the correlation functions to the rotation rate of the rigid protein. These reports have led us to develop a simple motional model for polyribonucleotides in their single- or double-stranded form. In the present model we define the spin-label as consisting of a nitroxide ring attached to a tether of variable length which itself is linked to the 4- or 5-position of the pyrimidine base through a sulfur bridge. We assign the fastest rotation to the pyrimidine–sulfur linkage, and we also assume substantial motion for the bases in single and double strands. This simple model allows us to analyze all the ESR data so far obtained on spin-labeled single- and double-stranded RNAs.

Other sources of motions, for instance the rotation of the spin-labeled RNA duplex as a whole, might contribute to the relaxation of the nitroxide. However, on the basis of hydrodynamic considerations a mean correlation time of 200 ns was calculated for a DNA molecule of 550 base pairs long rotating uniformly (Robinson et al., 1980b). By use of the same approach the present spin-labeled RNA duplexes consisting of about 300 base pairs should have a correlation time on the order of 100 ns. This value is by far larger than the correlation times measured for the spin-labeled nucleic acids, and therefore, the rotation of the spin-labeled RNA duplex as a whole can be neglected from the present motional model.

The present model supports the hypothesis of a rapid motion of the bases in the 4-ns time frame. Namely, $\tau_\perp$ can be due to (see Figure 2) torsion and tilting of the base pairs and twisting of the bases as well as to rotation of bond 2 or any bond parallel to it. The latter possibilities can be ruled out, because $\tau_\perp$ was found to be a constant and did not depend on the tether length. Thus, $\tau_\perp$ must reflect the mobility of the base which carries the spin-label. This conclusion is further strengthened by comparing the mobilities of the nitroxide labels in the single and corresponding double strands. Tables I and II show that for all systems $\tau_\perp$ is larger by a factor of 3.3 for the double strands than for the single strands. Such a difference would not be observable if the $\tau_\perp$ is caused by rotation around bond 2 or any bond parallel to it, since in such a case the same $\tau_\perp$ would have been obtained for single and double strands.

The observation that $\tau_\parallel$ varies in the case of the duplexes with the length of the tether fits the model. The nitroxide with the shortest tether displays as expected the largest $\tau_\parallel$, whereas the nitroxide with the longest tether has the shortest $\tau_\parallel$. With respect to the single strands $\tau_\parallel$ is small and exhibits nearly the same value in all cases, suggesting that in this mobility range the tether length will no longer affect $\tau_\parallel$. Spin-labeling in position 5 of U allows according to CPK models Watson–Crick type of base pairing in such a way that the spin-label can extend into the major groove of the duplex. On the other hand spin-labeling in position 4 should interfere with Watson–Crick type of base pairing, and a mobile nonintrahelical conformation of the spin-labeled nucleotide can be expected. A comparison of the mobilities of 5- vs. 4-spin-labeled nucleotides containing the same tether shows that both $\tau_\parallel$ and $\tau_\perp$ are larger by about a factor of 3 for the 5-substituted nucleotide in the presence of $(A)_n$ (Table II). As noted earlier all 5-substituted single strands display the same $\tau_\parallel$ and $\tau_\perp$ values, and those values are essentially the same as the $\tau_\parallel$ and $\tau_\perp$ values calculated for $(1s^4U,U)_n$ (Table I). Therefore, the substantial decrease in mobility for the 5-substituted $(U)_n$ as compared to the 4-substituted $(1s^4U,U)_n$ upon complexation strongly supports the hypothesis that 5-substituted bases assume intrahelical base pairing upon complexation with $(A)_n$. A similar conclusion was reached when comparing the correlation times of $(I)_n$-$(1s^4U,C)_n$ with those of $(A)_n(RUGT,U_{100})_n$ (Bobst et al., 1981b). Furthermore, the observed decrease in mobility in the case of $(RUTT,U)_n(A)_n$ supports the hypothesis that rotation around bond 2 or any bond parallel to it in the spin-label does not correspond to the dominant motion for $\tau_\perp$, or else the difference between a nonintrahelical and an intrahelical conformation could not have been observed.

In conclusion, this approach of analysis together with the present set of spin-labeled nucleic acids made it possible to separate the motion of the base from the spin-label motion. On the basis of the motional model which allows analysis of all the various RNA systems it is concluded that the bases in the RNA duplex experience substantial motions with a correlation time of a few nanoseconds.

Registry No. $(pps^5U)_2$, 87393-42-8; epoxy-Tempo, 53086-08-1; α-iodoacetamido-Tempo, 25713-24-0; β-iodoacetamido-Tempo, 87373-17-9; ppRUMMT, 87373-18-0; ppRUTT, 87373-19-1; ppRUMPT, 87373-20-4; $pp1s^4U$, 87373-21-5; $(RUMMT,U)_n$, 87373-24-8; $(RUTT,U)_n$, 87373-26-0; $(RUMPT,U)_n$, 87373-28-2; $(1s^4U,U)_n$, 87373-30-6; $(RUMMT,U)_n(A)_n$, 87373-32-8; $(RuTT,U)_n(A)_n$, 87373-34-0; $(RUMPT,U)_n(A)_n$, 87373-36-2; $(1s^4U,U)_n(A)_n$, 87373-37-3; 4-(β-chloropropanamido)-2,2,6,6-tetramethylpiperidinyl-1-oxy, 87373-22-6; 3-chloropropanoic acid, 107-94-8; 4-amino-2,2,6,6-tetramethylpiperidinyl-1-oxy, 14691-88-4.

References

Allison, S. A., Shibata, J. H., Wilcoxon, J., & Schurr, J. M. (1982) *Biopolymers 21*, 729–762.

Berliner, L. J. (1976) *Spin Labeling: Theory and Applications*, Academic Press, New York.

Bobst, A. M. (1979) in *Spin Labeling II: Theory and Applications* (Berliner, L. J., Ed.) pp 291–345, Academic Press, New York.

Bobst, A. M. (1980) in *Molecular Motion in Polymers by ESR* (Boyer, R. F., & Keinath, S. E., Eds.) pp 167–175, Harwood Academic Publishers, New York.

Bobst, A. M., Ireland, J. C., & Langemeier, P. W. (1981a) *Biophys. J. 33*, 313a.

Bobst, A. M., Langemeier, P. W., Torrence, P. F., & Declercq, E. (1981b) *Biochemistry 20*, 4798–4803.

Bolton, P. H., & James, T. L. (1979) *J. Phys. Chem. 83*, 3359–3366.

Feigon, J., & Kearns, D. R. (1979) *Nucleic Acids Res. 6*, 2327–2337.

Freed, J. H. (1976) in *Spin Labeling: Theory and Applications* (Berliner, L. J., Ed.) pp 53–132, Academic Press, New York.

Goldman, S. A., Bruno, G. V., Polnaszek, C. F., & Freed, J. H. (1972) *J. Chem. Phys. 56*, 716–735.

Griffith, O. H., Cornell, D. W., & McConnell, H. M. (1965) *J. Chem. Phys. 43*, 2909–2910.

Hakam, A., Thomas, I. E., & Bobst, A. M. (1980) *Int. J. Biol. Macromol. 2*, 49–51.

Ho, Y. K., Novak, L., & Bardos, T. J. (1978) in *Nucleic Acid Chemistry* (Townsend, S. B., & Tipson, R. S., Eds.) Part II, pp 813-816, Wiley, New York.
Hogan, M. E., & Jardetzkey, O. (1980) *Biochemistry 19*, 3460-3468.
Hogan, M. E., Wang, J., Austin, R. H., Monitto, C. L., & Hershkowitz, S. (1982) *Proc. Natl. Acad. Sci. U.S.A. 79*, 3518-3522.
Hurley, I., Osei-Gyimah, P., Archer, S., Scholes, C. P., & Lerman, L. S. (1982) *Biochemistry 21*, 4999-5009.
Klevan, L., Armitage, I. M., & Crothers, D. M. (1979) *Nucleic Acids Res. 6*, 1607-1616.
Langemeier, P. W., & Bobst, A. M. (1981) *Arch. Biochem. Biophys. 208*, 205-211.
Luoma, G. A., Herring, F. G., & Marshall, A. G. (1982) *Biochemistry 21*, 6591-6598.
Mason, R. P., Polnaszek, C. F., & Freed, J. H. (1974) *J. Phys. Chem. 78*, 1324-1329.
McCain, D. C., Virudachalam, R., Santini, R. E., Abdel-Meguid, S. S., & Markley, J. L. (1982) *Biochemistry 21*, 5390-5397.
Meirovitch, E., Igner, D., Igner, E., Moro, G., & Freed, J. H. (1982) *J. Chem. Phys. 77*, 3915-3938.
Ozinskas, A. J., & Bobst, A. M. (1979) *Helv. Chim. Acta 62*, 1677-1681.
Ozinskas, A. J., & Bobst, A. M. (1980) *Helv. Chim. Acta 63*, 1407-1411.
Polnaszek, C. F. (1976) Ph.D. Thesis, Cornell University, Ithaca, NY.
Polnaszek, C. F., & Freed, J. H. (1975) *J. Phys. Chem. 79*, 2283-2306.
Polnaszek, C. F., Schreier, S., Butler, K. W., & Smith, I. C. P. (1978) *J. Am. Chem. Soc. 100*, 8223-8232.
Rauckman, E. J., Rosen, G. M., & Abou-Donia, M. B. (1976) *Org. Prep. Proced. Int. 8*, 159-161.
Robinson, B. H., & Dalton, L. R. (1980) *J. Chem. Phys. 72*, 1312-1324.
Robinson, B. H., Forgacs, G., Dalton, L. R., & Frisch, H. L. (1980a) *J. Chem. Phys. 73*, 4688-4692.
Robinson, B. H., Lerman, L. S., Beth, A. H., Frisch, H. L., Dalton, L. R., & Auer, C. (1980b) *J. Mol. Biol. 139*, 19-44.
Shindo, H., & McGhee, J. D. (1980) *Biopolymers 19*, 523-537.
Toppin, C. R. (1983) Ph.D. Thesis, University of Cincinnati, Cincinnati, OH.
Wallach, D. (1967) *J. Chem. Phys. 47*, 5258-5268.
Wang, J., Hogan, M. E., & Austin, R. H. (1982) *Proc. Natl. Acad. Sci. U.S.A. 79*, 5896-5900.
Warwick, P. E., Hakam, A., Bobst, E. V., & Bobst, A. M. (1980) *Proc. Natl. Acad. Sci. U.S.A. 77*, 4574-4577.

Phycocyanin 612: A Biochemical and Photophysical Study†

Robert MacColl* and Deborah Guard-Friar

ABSTRACT: Phycocyanin 612 was isolated from the cryptomonad *Hemiselmis virescens* and purified. Sedimentation equilibrium experiments indicated a molecular weight of 56 000, and sodium dodecyl sulfate gel electrophoresis yielded two bands of molecular weight 10 000 (α) and 18 000 (β) in a 1:1 molar ratio. A quaternary structure of $\alpha_2\beta_2$ was confirmed by sodium dodecyl sulfate gel electrophoresis after cross-linking the protein with dimethyl suberimidate. Analysis of the absorption spectrum of phycocyanin 612 in acidic urea showed that the protein has two types of tetrapyrrole chromophores: phycocyanobilin, A_{max} at 662 nm, and cryptoviolin, A_{max} at 590 nm. The $\alpha_2\beta_2$ structure has six phycocyanobilins and two cryptoviolin chromophores. The α and β subunits were completely separated by chromatography on a Sephacryl S-200 column in acidic urea. The α subunit has only phycocyanobilin; the β has both phycocyanobilin and cryptoviolin in a 2:1 ratio. Comparison of the total amounts of separated subunits produced a molar ratio of α to β phycocyanobilin of 1:2 and of α phycocyanobilin to β cryptoviolin of 1:1. The distribution of chromophores is then one phycocyanobilin per α subunit and two phycocyanobilins and one cryptoviolin per β. Fluorescence and fluorescence-polarization spectroscopy demonstrated very efficient excitation-energy transfer from the cryptoviolins to phycocyanobilins. Circular dichroism spectroscopy indicated that the phycocyanobilins were split, either by strong exciton coupling or by different tetrapyrrole conformations, into at least two types. Both the cryptoviolins and phycocyanobilins were in a more extended conformation in the native state, compared to their cyclic conformation in the denatured state.

Cryptomonads are flagellated protozoa that perform photosynthesis through a unique array of pigments: biliproteins, chlorophyll c_2, and chlorophyll *a*. Biliproteins are chromoproteins that have covalently bound linear tetrapyrrole chromophores that also occur in blue-green and red algae. The biliproteins from these sources have been studied much more extensively than those from the cryptomonads [for reviews, see Gantt (1979, 1981), Scheer (1981), and Troxler (1977)].

There are six spectroscopic classes of cryptomonad biliproteins—three phycocyanins and three phycoerythrins (O'hEocha et al., 1964)—with one class per organism. Although allophycocyanin has not yet been discovered in any cryptomonad, it occurs in several forms in all blue-green and red algae (Zilinskas et al., 1978; Troxler et al., 1980), where it has a vital function (Gantt et al., 1976; Gantt & Lipschultz, 1973). Three types of cryptomonad biliprotein—phycocyanin 645, phycoerythrin 545, and phycoerythrin 565—have been carefully investigated (Brooks & Gantt, 1973; Glazer & Cohen-Bazire, 1975; Glazer et al., 1971; Jung et al., 1980; MacColl et al., 1973, 1976; Mörschel & Wehrmeyer, 1975, 1977), while the remaining cryptomonad biliproteins including

† From the Center for Laboratories and Research, New York State Department of Health, Albany, New York 12201. *Received May 17, 1983.* This research was supported by NIH Grant GM 26050 awarded by the National Institute of General Medical Science, U.S. PHS, DHHS.

0006-2960/83/0422-5568$01.50/0